Solid Earth Discuss., 6, 2645–2674, 2014
www.solid-earth-discuss.net/6/2645/2014/
doi:10.5194/sed-6-2645-2014
© Author(s) 2014. CC Attribution 3.0 License.

Solid Earth Discussions
Open Access

This discussion paper is/has been under review for the journal Solid Earth (SE).
Please refer to the corresponding final paper in SE if available.

Tunable diode laser measurements of hydrothermal/volcanic CO_2, and implications for the global CO_2 budget

M. Pedone[1], A. Aiuppa[1,2], G. Giudice[2], F. Grassa[2], V. Francofonte[2], B. Bergsson[1,3], and E. Ilyinskaya[4]

[1]DiSTeM, Università di Palemo, via Archirafi, 36, Palermo 90123, Italy
[2]Istituto Nazionale di Geofisica e Vulcanologia, Sezione di Palermo, via Ugo La Malfa, 153, Palermo 90146, Italy
[3]Icelandic Meteorological Office, Bústaðavegur 7, Reykjavík, Iceland
[4]British Geological Survey, Murchison House, West Mains Road, Edinburgh, EH91QZ, UK

Received: 1 August 2014 – Accepted: 6 August 2014 – Published: 27 August 2014

Correspondence to: M. Pedone (maria.pedone@unipa.it)

Published by Copernicus Publications on behalf of the European Geosciences Union.

Abstract

Quantifying the CO_2 flux sustained by low-temperature fumarolic fields in volcanic-hydrothermal environment has remained a challenge, to date. Here, we explored the potentiality of a commercial infrared tunable laser unit for quantifying such fumarolic volcanic/hydrothermal CO_2 fluxes. Our field tests were conducted (between April 2013 and March 2014) at Nea Kameni (Santorini, Greece), Hekla and Krýsuvík (Iceland) and Vulcano (Aeolian Islands, Italy). At these sites, the tunable laser was used to measure the path-integrated CO_2 mixing ratios along cross-sections of the fumaroles' atmospheric plumes. By using a tomographic post-processing routine, we then obtained, for each manifestation, the contour maps of CO_2 mixing ratios in the plumes and, from their integration, the CO_2 fluxes. The so-calculated CO_2 fluxes range from low ($5.7 \pm 0.9\,t\,day^{-1}$; Krýsuvík) to moderate ($524 \pm 108\,t\,day^{-1}$; "La Fossa" crater, Vulcano). Overall, we suggest that the cumulative CO_2 contribution from weakly degassing volcanoes in hydrothermal stage of activity may be significant at global scale.

1 Introduction

The chemical composition of volcanic gas emissions can provide hints onto the mechanisms of magma ascent, degassing and eruption (Allard et al., 2005; Burton et al., 2007; Oppenheimer et al., 2009, 2011), and can add useful information for interpreting the dynamics of fluid circulation at dormant volcanoes (Giggenbach, 1996; Chiodini et al., 2003, 2012).

Carbon dioxide (CO_2) is, after water vapour, the main constituent of volcanic (Giggenbach, 1996) and hydrothermal (Chiodini et al., 2005) gases, and has attracted the attention of volcanologists because it can contribute to tracking magma ascent prior to eruption (Aiuppa et al., 2007, 2010). The volcanic/hydrothermal CO_2 flux sustained by diffuse soil degassing can be measured relatively easily during surveys (Chiodini et al., 1996, 2005; Favara et al., 2001; Hernández, 2001; Cardellini et al., 2003; Inguag-

giato et al., 2005, 2012; Pecoraino et al., 2005; Mazot et al., 2011) or with permanent installations (Brusca et al., 2004; Carapezza et al., 2004; Werner and Cardellini, 2006; Inguaggiato et al., 2011). In contrast, the volcanic CO_2 flux contributed by open vents and/or fumarolic fields is more difficult to measure, since the volcanic gas CO_2 signal is diluted – upon atmospheric transport – into the overwhelming background air CO_2 signal. Such volcanic CO_2 flux emissions have been quantified for only ∼30 volcanic sources, based upon simultaneous measurement of SO_2 fluxes (via UV spectroscopy) and CO_2/SO_2 plume ratios (via direct sampling, Fourier transform Infra Red (FTIR) spectroscopy, or the Multi-GAS; see Burton et al., 2013). This methodology is however not applicable to the countless number of quiescent volcanoes with low-temperature (SO_2-free) emissions (Aiuppa et al., 2013). As a consequence, the available dataset of volcanic CO_2 fluxes is still incomplete, making estimates of the global volcanic CO_2 flux poorly accurate (Burton et al., 2013).

In this paper, we discuss the use of Tunable Diode Laser Spectrometers (TDLS) for estimating volcanic/hydrothermal CO_2 fluxes from quiescent volcanoes. Tunable Diode Lasers are increasingly used in air monitoring (Gianfrani et al., 1997a) and, more recently, for volcanic gas observations (Gianfrani et al., 1997b, 2000; De Natale et al., 1998; Richter, 2002). Pedone et al. (2014), recently reported on the first direct observation of the volcanic CO_2 flux from the fumaroles of Campi Flegrei (southern Italy), by using a portable Tunable Diode Laser (TDL) system.

We here extend this previous work, discussing the results of TDL observations at four additional quiescent volcanoes: Nea Kameni (Santorini, Greece), Hekla and Krýsuvík (Iceland), and Vulcano Island (Aeolian Islands, Italy) (Fig. 1). We select these volcanoes because they display a range of fumarolic activity from weak (Krýsuvík, Hekla) to moderate (Vulcano Island). While there is strong argument for the global volcanic CO_2 budget being dominated by a relatively small number of strong emitters (Shinohara, 2013), it remains that weakly degassing volcanoes dominate – at least in number – the population of historically active volcanoes on Earth. It is on characterising the typical

levels of CO_2 emission from such feeble volcanic point sources that we concentrate on in this study.

2 Background

Santorini, the site of the famous Minoan eruption ∼3600 yr ago (Druitt et al., 1999), is an island located in the Aegean Sea, part of the Ciclades Archipelago. Santorini has a surface of 75.8 km^2 and is presently made up of five islands (Thera, Therasia, Aspronisi, Palea Kameni and Nea Kameni) that constitute the active intra-caldera volcanic field (Dominey-Howes and Minos-Minopulos, 2004). Four periods of unrest in the 20th century have culminated into small-scale eruptions in 1925–1926, 1928, 1939–1941 and 1950 (Fyticas et al., 1990; ISMOSAV, 2009). Outside the caldera, volcanic activity has been recorded in 1649–1650 AD, in the Kolumbo submarine volcano (Vougioukalakis et al., 1994). Since the last eruption in 1950, the volcano has remained quiescent (Tsapanos et al., 1994; Papazakos et al., 2005; ISMOSAV, 2009). In early 2011, geodetic monitoring revealed an new stage of caldera-wide uplift (Newman et al., 2012; Parks et al., 2012), accompanied by swarms of shallow earthquakes. This unrest lasted from January 2011 to April 2012 (Parks et al., 2013). Degassing activity at Santorini is currently concentrated in a small, hydrothermally altered area on top of Nea Kameni islet (Parks et al., 2013), where a number of weakly fuming fumaroles (mostly CO_2, water vapour and air-derived gases; temperatures of 93–97 °C) are concentrated (Tassi et al., 2013). A recent survey carried by Parks et al. (2013) indicated increased diffuse CO_2 emissions between September 2010 and January 2012; this period was characterized by a change in the degassing pattern, with an increase in soil CO_2 emissions peaking at $38 \pm 6\,t\,d^{-1}$ in January 2012 (Parks et al., 2013). Tassi et al. (2013) examined the response of fumarole composition to the 2011–2012 unrest, and reported increasing CO_2 concentrations (and decreasing $\delta^{13}C-CO_2$) from May 2011 to February 2012, suggesting mantle CO_2 contribution. The summit fumarolic field was the site of our 9 April 2013 survey (see Figs. 1a and 2).

Hekla is one of the most active volcanoes in Europe. Its historical volcanic activity, petrology and geochemistry of volcanic rocks have been the subject of several studies (e.g. Thorarinsson, 1967; Sigmarsson, 1992). Hekla (63.98° N, 19.70° W; 1490 m a.s.l.) is located in the southern part of Iceland at the intersection of the South Iceland Fracture Zone and the Eastern Volcanic Zone (Thordarsson and Larsen, 2007 and references cited). Five plinian eruptions have been identified in the historical record, most recently in 1104 AD (Thorarinsson, 1967; Larsen et al., 1999). In recent decades, Hekla has erupted frequently, at an average rate of one eruption per decade, and most recently in 2000 (Höskuldsson et al., 2007). Gas information has long remained missing, because Hekla appears to be only degassing during eruptions. Very recently, Ilyinskaya et al. (2014) identified a weakly degassing, warm ground on the summit of the Hekla 1980–1981 crater (Fig. 1b), and studied the composition of this gas using data from a permanent Multi-GAS instrument and field campaigns using an accumulation chamber installed by INGV-PA (Istituto Nazionale di Geofisica e Vulcanologia, Sezione di Palermo) and IMO (Icelandic Meteorological Office) in 2012. These authors provided evidences for this gas spot being the only current surface manifestation at Hekla. This degassing field was therefore the site of our measurement survey with the TDL on 2 July 2013 (see Figs. 1b and 3).

Krýsuvík (Fig. 1c) is one of five presently active geothermal areas on the Reykjanes Peninsula, in Iceland (Markússon and Stefansson, 2011). Geothermal activity at Krýsuvík includes hot grounds, steaming vents, steam-heated hot springs and mud pots, and pervasive surface alteration. The most important surface manifestations are confined to the Sveifluháls area, including Austurengjahver and the small areas of Seltún and Hveradalur (Markússon et al., 2011). On 5 July 2013, we performed TDL observations in Hveradalur (63°53,449′ N, 22°4,190′ W; Figs. 1c and 4). This area included two major fumarolic manifestations (indicated as "FumA" and "FumB" in Fig. 4). The fumarolic vent "FumA" is monitored by a permanent Multi-GAS instrument (shown as a triangle in Fig. 4) deployed in a joint monitoring program led by British Geological Survey (BGS), INGV and IMO.

Vulcano is a volcanic island belonging to the Aeolian Islands in the southern Tyrrhenian Sea (Italy). Since the last eruption in 1888–1890, this closed-conduit volcanic system has been characterized by intense fumarolic activity concentrated on the summit of La Fossa crater (Fig. 1d), a small (391 m a.s.l.; 2 km in diameter) < 5 ka old pyroclastic cone. Degassing activity has shown signs of intensification in the last decades, including increased fumarole temperatures (Badalamenti et al., 1991; Chiodini et al., 1995; Capasso et al., 1997), and episodic variations of gas/steam ratios (Chiodini et al., 1996; Capasso et al., 1999; Paonita et al., 2002, 2013). The CO_2 flux from the La Fossa fumarolic field has been measured previously by Aiuppa et al. (2005, 2006), McGonigle et al. (2008), Tamburello et al. (2011) and Inguaggiato et al. (2012). On 11 March 2014, we measured the CO_2 emissions from La Fossa using the measurement configuration of Fig. 1d.

3 Methods

The Tunable Diode Laser Spectroscopy technique (TDLS) relies on measuring the absorbance due to the absorption of IR radiation (at specific wavelengths) by a target gas. Like in previous work at Campi Flegrei (Pedone et al., 2014), we used a GasFinder 2.0 Tunable Diode Laser (produced by Boreal Laser Inc.), a transmitter/receiver unit that can measure CO_2 mixing ratios over linear open-paths of up to 1 km distance, operating in the 1.3–1.7 µm wavelength range. Radiation emitted by the IR laser transmitter propagates to a gold plated retro-reflector mirror, where it is reflected back to the receiver and focused onto a photodiode detector. Incoming light is converted into electrical waveform, and processed to determine in real-time the linear CO_2 column amount (in ppm m) along the optical path, using the procedure described in Tulip (1997). CO_2 column amounts are converted into average CO_2 mixing ratios (in ppm) along the path by knowledge of path lengths (measured with an IR manual telemeter, 1 m resolution). A portable meteorological station was continuously recording (frequency = 1 Hz) during the measurements to restrict post-processing to sampling intervals characterized

by similar meteorological conditions. Instrumental accuracy is evaluated using a correlation coefficient (R^2), which is a measure of the similarity between the waveforms of the sample and reference signals. According to manufacture's datasheets, an accuracy of ± 2 % is achieved for $R^2 > 0.95$ (Trottier et al., 2009).

In the field, the GasFinder was set to measure CO_2 mixing ratios at 1 Hz rate (Pedone et al., 2014). Alignment between the laser unit and the retro-reflector mirror was optimised using a red visible aiming laser and a sighting scope. The size of the retro-reflector mirror was chosen as to adjust the returning light level to a desired value, depending on the path-length and the expected amount of absorbed radiation.

4 Results and discussions

4.1 Field operations

The GasFinder operated for more than 10 h during the four field campaigns (more than 4 h at Nea Kameni on 9 April 2013; 1 h at Hekla on 2 July 2013; 1.5 h at Krýsuvík on 5 July 2013; and more than 2 h at Vulcano on 11 March 2014). Measuring at 1 Hz, the GasFinder acquired more than 9000 readings of path-integrated CO_2 mixing ratios. However, we concentrate here onto a subset of data (1070 readings for Nea Kameni; 985 readings for Hekla; 1150 readings for Krýsuvík and 1757 for Vulcano Island), extracted from the original dataset based on data quality criteria (the same described in Pedone et al., 2014): we selected readings characterized by high accuracy (R^2 values > 0.95, optimal light values), and taken during phases of stable wind direction and speed. Northern trending winds prevailed during the field campaign at Nea Kameni (red arrow in Fig. 2); southern trending winds at Hekla (red arrow in Fig. 3); and north-western trending winds at both Krýsuvík (red arrows in Fig. 4) and "La Fossa" crater at Vulcano Island (red arrow in Fig. 5).

Figure 1 shows the GasFinder operational field set-up at the four volcanoes. In each picture, the GasFinder unit positions are expressed by letters; while retro-reflectors

positions are expressed by numbers (Fig. 1). During each campaign, and at each of the degassing areas, the position of the GasFinder unit was sequentially moved (e.g., from positions A to F in Fig. 1a) so as to scan the plume from different viewing directions and angles. We acquired along each single GasFinder – retro-reflector path (e.g., path A-1 in Fig. 1a) for ~ 4–5 min, before rotating the instrument' head to measure along the successive path (e.g., A-2). The number of operated paths ranged from 9 (Hekla) to 36 (Nea Kameni and Vulcano), and the entire measurement grid (e.g., the total number of possible Gas-Finder – retro-reflector paths) was covered in a few hours at most.

4.2 CO_2 mixing ratios and plume transport speed

The highest CO_2 mixing ratios (~ 1050 ppm) were measured at Hekla (Fig. 3), while the lowest mixing ratios values were detected at Nea Kameni and Krýsuvík (peaking at 590 ppm and < 500 ppm respectively, see Figs. 2 and 4). Intermediate CO_2 mixing ratios (~ 900 ppm) were detected at "La Fossa" crater at Vulcano Island (Fig. 5), reflecting gas contribution from fumarolic vents located on the rim and in the inner wall of the crater.

Background readings were obtained in each of the measurement sites by pointing the laser beam toward a mirror, positioned upwind the fumarolic area (Pedone et al., 2014). Background values of < 400 ppm were observed in all the analysed areas (Figs. 2–5).

During each campaign, the vertical plume transport speed was measured by a video camera pointing toward the fumarolic vents, and acquiring sequences of images of the atmospheric plume at 25 frames per second (see Aiuppa et al., 2013; Pedone et al., 2014). The sequences of frames were later post-processed to calculate the time-averaged plume transport speed, after converting camera pixels into distances (using a graduated pole, positioned close to the vent). Plume transport vertical speeds are reported in Table 1, and converge at 1–1.2 m s^{-1} at all volcanoes.

4.3 Contouring of in-plume CO_2 mixing ratios

At each of the four volcanoes, we combined the available set of path-integrated mixing ratio data to derive a two-dimensional reconstruction of CO_2 distribution (in ppm) in the plume cross-section, between the GasFinder position(s) and the retro-reflectors.

To this aim, we used a Matlab script (released by the authors, and available on request; see Pedone et al., 2014 for more details), to (i) create a matrix containing information on the geometry of the experimental setup (an example is given in Fig. 2 for Nea Kameni) and (ii) use this matrix to obtaining a bi-dimensional reconstruction of CO_2 concentrations in a cross-section of the atmospheric plumes, starting from the raw GasFinder dataset. In order to start the calculations, the Matlab script was initialised with the coordinates of laser and retro-reflectors positions. The additional input data was a column vector, containing the mean CO_2 column amount (in ppm m) obtained for the different GasFinder-retro-reflector paths. With these inputs, the script performed a data inversion using a least-squared method, previously described by Pedone et al. (2014). The geometric matrix (Fig. 2a) generated by the Matlab algorithm, is a geometric reconstruction of the experimental set-up (the explored space was dived into 16 equally sized cells; the red cells in Fig. 2a). The scripts used the data inversion procedure to assign an averaged CO_2 mixing ratio (in ppm) to each cell of the 4×4 matrix (the same 16 cells of Fig. 2a). Using sets of synthetic data to test the algorithm, we estimated an error of $\leq 3\,\%$ associated to these individual cell mixing ratios.

The so-called tomographic matrix (Fig. 2b) was then interpolated with the Surfer software to obtain the contour maps of Figs. 2c and 3–5. We used the Point Kriging geo-statistical method to interpolate the available data and produce an interpolated grid (Isaaks and Srivastava, 1989). Figure 2c is the contour map of CO_2 mixing ratios obtained at Nea Kameni. This map (obtained by interpolation of the tomographic matrix of Fig. 2b) shows the distribution of CO_2 mixing ratios in the roughly horizontal atmospheric cross-section, covering the area between the Gas Finder (A–F) and retro-reflector (1–6) positions (Fig. 1a). The figure shows that, in spite of the feeble

degassing activity present, a CO_2 plume is imaged by our observations on the eastern, inner rim of the Nea Kameni crater. Low CO_2 mixing ratios (~ 390 ppm) are outputted by the Matlab routine on the north-western portion of the investigated area, while higher CO_2 mixing ratios (from 490 to ~ 540 ppm) are identified on the east, where the main gas emission vents are located. The peak CO_2 mixing ratio of ~ 590 ppm is located in correspondence to one principal gas vent (marked as "Fum6" in Fig. 2c).

Similar results have been obtained at Hekla, Krýsuvík and Vulcano. Figure 3 is a contour map of CO_2 mixing ratios at the Hekla measurement site (Fig. 1b). Given the positioning of Gas Finder and retro-reflectors, the Matlab-derived contour map is here relative to an hypothetical horizontal cross-section, taken at about 1 m height above the warm degassing ground identified by Ilyinskaya et al. (2014) on the rim of the 1980–1981 summit crater of Hekla (Figs. 1b and 3). In this area, the background CO_2 mixing ratio was evaluated at around 400 ppm. The peak CO_2 mixing ratio (~ 1050 ppm) was detected in the central portion of the investigated area, in the same sector where the highest soil CO_2 fluxes have been observed (Ilyinskaya et al., 2014).

The CO_2 contour map obtained at Krýsuvík is shown in Fig. 4. In this area, CO_2 mixing ratios ranged from 350–380 ppm at the periphery of the exhaling area, and up to ~ 500 ppm near the two main fumarolic vents ("FumA" and "FumB" in Fig. 4).

The CO_2 distribution map of "La Fossa" crater at Vulcano Island is shown in Fig. 5. The highest CO_2 mixing ratios (up to 880 ppm; Fig. 5) were detected in correspondence of the principal fumaroles ("F0", "F5" and "F11") of the crater rim and the "FA" fumarolic field in the inner wall of the crater.

4.4 Calculation of the CO_2 flux

The ability of the TDL to contour CO_2 mixing ratios in a volcanic gas plume cross section (Figs. 2–5) opens the way to quantification of the fumarolic CO_2 output from each of the studied areas.

In order to calculate the CO_2 output from each fumarolic area, we integrated each set of CO_2 mixing ratio values in each CO_2 contour map (Figs. 2–5), to obtain a CO_2

Integrated Column Amount (ICA) over the entire plume cross-section. This ICA was then multiplied by the vertical plume transport speed, yielding a CO_2 flux. The calculated CO_2 fluxes are listed, for each site and each campaign, in Table 1. The accuracy (1 σ) of the mean flux estimates are calculated from error propagation theory applied to both ICA and plume transport vertical speed.

Applying this procedure to the contour map of Fig. 2, we estimate a CO_2 flux from Nea Kameni fumaroles of $63 \pm 22\,\mathrm{t\,day^{-1}}$. This fumarolic output is ~ 4 times higher than the total diffuse discharge from the soils of $15.4\,\mathrm{t\,day^{-1}}$ reported by Chiodini et al. (1998), and ~ 1.5 times higher than the soil CO_2 output of $38 \pm 6\,\mathrm{t\,day^{-1}}$ estimated (in January 2012) by Parks et al. (2013). We conclude that the weak but persistent fumarolic activity on-top of Nea Kameni is the major emission source of CO_2 at this volcano.

For Hekla, we estimated a CO_2 flux of about $15 \pm 7\,\mathrm{t\,day^{-1}}$ (Table 1). The large error in our flux estimate (±46 %) is here reflecting the poor quality of our plume transport speed measurement, which determination was complicated by the strong winds blowing on top of Hekla by the time of our measurements. We still observe, however, that our $15 \pm 7\,\mathrm{t\,day^{-1}}$ estimate matches closely the recently reported CO_2 flux for Hekla summit ($13.7 \pm 3.7\,\mathrm{t\,day^{-1}}$), obtained using conventional (accumulation chamber) soil survey techniques (Ilyinskaya et al., 2014).

For the Hveradalur fumarolic field of Krýsuvík, we estimate a CO_2 flux of $5.7 \pm 0.9\,\mathrm{t\,day^{-1}}$ (Table 1). This is the first CO_2 output estimate for this area, at least to our knowledge.

Finally, on March 2014 we evaluate the CO_2 flux at La Fossa crater at $524 \pm 108\,\mathrm{t\,day^{-1}}$ which is in the same range of those obtained in previous studies by Aiuppa et al. (2005) ($420 \pm 250\,\mathrm{t\,d^{-1}}$), Tamburello et al. (2011) ($488\,\mathrm{t\,d^{-1}}$, average of two campaigns in 2009) and Inguaggiato et al. (2012) ($453\,\mathrm{t\,d^{-1}}$) (see Fig. 6) and using different techniques.

4.5 Implications for the global volcanic CO_2 flux

Our CO_2 observations were taken at four volcanoes displaying a range of fumarolic activity, from weak (Hekla) to moderately strong (La Fossa of Vulcano). As such, our results add novel information on the CO_2 degassing regime of quiescent volcanoes in Solfatara stage of activity, and on their potential contribution to the global volcanic CO_2 budget.

The current state-of-the-art of volcanic CO_2 flux research has recently been summarised in Burton et al. (2013). The authors presented a compilation of 33 subaerial volcanoes for which CO_2 flux observations were available at that time. These "measured" emissions totalled a cumulative CO_2 output of $59.7\,\mathrm{Mt\,yr^{-1}}$. The same authors used linear extrapolation, from the measured 33 to the 150 plume-creating, passively degassing volcanoes on the GVP catalogue (Siebert and Simkin 2002), to obtain an extrapolated global volcanic CO_2 flux of $\sim 271\,\mathrm{Mt\,yr^{-1}}$.

The linear extrapolation approach of Burton et al. (2013) is based on the implicit assumption that the measured 33 volcanoes represent a statistically significant sub-set of the volcanic CO_2 flux population. However, we argue that past volcanic CO_2 observations have been prioritized at strongly degassing volcanoes under unrests; therefore, the 33 volcanoes population may be biased towards the category of top gas emitter, implying the linear extrapolation technique may be incorrect. The low CO_2 output associated to "quiet" volcanoes, as reported in our present work, corroborates this conclusion.

The alternative extrapolation approach used to quantify CO_2 emissions from "unmeasured" volcanoes is to assume that the distribution of volcanic CO_2 fluxes obeys a power law (Brantley and Koepenick, 1995), as other geophysical parameters do (Marret and Allmendinger, 1991; Turcotte, 1992). If volcanic emissions follow a power-law distribution, then the number of volcanoes (N) with an emission rate $\geq f$ are given by:

$$N = af^{-c} \quad (1)$$

where a and c are constants that can be derived from linear regression on measured CO_2 emission datasets. In the power-law assumption, the global volcanic CO_2 flux (f_{tot}) was extrapolated to 88–132 Mt yr^{-1} (Brantley and Koepenick, 1995) using the relation:

$$f_{tot} = f_1 + f_2 + f_3 + f_N \left[\frac{c}{1-c}(N+1) \left(\frac{N}{N+1} \right)^{\frac{1}{c}} \right] \quad (2)$$

where f_N refers to the Nth-largest measured flux. This 88–132 Mt yr^{-1} estimate is a factor 2–3 lower than obtained with the linear extrapolation technique (Burton et al., 2013). On the same basis, the volcanic+metamorphic CO_2 flux was evaluated at ~ 264 Mt yr^{-1} (Brantley and Koepenick, 1995).

The power-law distribution assumption has extensively been used to extrapolate volcanic gas fluxes at both global and individual-arc scale (Hilton et al., 2002). However, concerns have recently been raised on its validity. For example, Mori et al. (2013) demonstrated that the SO_2 flux distribution of Japanese volcanoes noticeably diverges from a simple power law distribution. The case of the global volcanic CO_2 flux population is illustrated in Fig. 7. The figure is a log-log plot of the cumulative number of volcanoes (N) having measured CO_2 flux of $\geq f$. The diagram is based upon the dataset of Burton et al. (2013), implemented with new results from this study (Table 1) and additional data for Turrialba (1140 t day^{-1}; Conde et al., 2014) and Poas (24.7 t day^{-1}; Aiuppa et al., 2014) in Costa Rica, Telica (132 t day^{-1}; Conde et al., 2014) and San Cristobal (523 t day^{-1}; Aiuppa et al., 2014) in Nicaragua, Lastarria (973 t day^{-1}) and Láscar (534 t day^{-1}) in Chile (Tamburello et al., 2013), and Soufriere in Guadeloupe (14.9 t day^{-1}; Allard et al., 2014). This implemented CO_2 flux population (43 volcanoes in total) clearly departs from a linear trend, as would be expected for a power-law distribution (see Eq. 1). The observed distribution shows, instead, a clear inflection point at log f ~ 2.5–2.8 (e.g., CO_2 flux of ~ 300–600 t day^{-1}), which appears to divide high (> 600 t day^{-1}) from low (< 300 t day^{-1}) CO_2 flux volcanoes (L and H regression lines in Fig. 7).

In view of our novel results (listed in Table 1), we propose that the non-linear behavior of the volcanic CO_2 flux population may (at least in part) reflect the scarcity of CO_2 flux information on weakly fuming, quiescent volcanoes. The case Hekla is emblematic in this context: the volcano has remained in a very active state in the last century (it violently erupted only fourteen years ago; Höskuldsson et al., 2007), but shows today no visible plume or gas emission. Yet however, our data suggest the volcano may contribute daily ~ 15 t of CO_2 to the atmosphere in invisible, but probably persistent form. Similarly, no plume is seen on top of Nea Kameni in Santorini, which weak fumaroles yet release 63 ± 22 t of CO_2 every day (in addition to a sizeable diffuse contribution from the soil), and 5.7 ± 0.9 t of CO_2 are released daily by quiet hydrothermal activity at Krýsuvík (which most recent activity probably dates back the 14th century; Smithsonian Institute, 2013). While the individual contribution of each of the above volcanoes is negligible globally, the cumulative contribution of all feebly degassing volcanoes on Earth may not, and may impact the global CO_2 flux distribution of Fig. 7.

To explore the latter argument further, we consider that, of the 1549 volcanic structures listed in the GVP catalogue, around 500 are considered to have been active in the Holocene (Smithsonian Institution, 2013), and thus still potentially degassing. For the sake of illustration, we assume that all such 500 volcanoes have a CO_2 flux equal to or higher than 10 t day^{-1} (the mean of our measured Krýsuvík and Hekla fluxes). This yields to a new point in Fig. 7, with coordinates log f = 1 (CO_2 flux = 10 t day^{-1}) and log N = 2.69 (500 volcanoes), which lies right above the linear regression line of the high CO_2 flux (log f > 2.5) population (see dashed line H in Fig. 7). The regression line (line H_1; R^2 = 0.98) obtained considering the high CO_2 flux volcanoes (log $f \geq 2.5$) plus this new log f = 1 point has slope c = −0.72. Using this value in Eq. (2), and with N = 500, we calculated an extrapolated CO_2 flux of 67 Mt yr^{-1}. From these preliminary calculations, we conclude that (i) the power-law distribution may be an appropriate representation of the population of CO_2 flux data, provided the output of the several hundreds of weakly degassing, quiescent/hydrothermal/dormant volcanoes is considered;

(ii) a large number of volcanoes remain to be measured, possibly being characterized by intermediate CO_2 output ($\log f$ between 1 and 2.5 in Fig. 7).

5 Conclusions

We have investigated the fumarolic CO_2 output from 4 quiescent volcanoes in hydrothermal state of activity, using an Infra Red TDL. At each of the studied volcanoes, the acquired TDL results have been used to contour CO_2 mixing ratios in the plumes' cross-sections, and consequently to quantifying the fumarolic CO_2 output. The highest output ($524 \pm 108\,\mathrm{t\,day^{-1}}$) is obtained at La Fossa of Vulcano Island, the only volcano of the 4 where a persistent atmospheric plume is observed. The lowest CO_2 output ($5.7 \pm 0.9\,\mathrm{t\,day^{-1}}$) is associated with hydrothermal activity at Krýsuvík, with intermediate emissions at Hekla ($15 \pm 7\,\mathrm{t\,day^{-1}}$) and Nea Kameni ($63 \pm 22\,\mathrm{t\,day^{-1}}$). The latter 3 volcanoes all currently display weak exhalative activity and no visible plume emission. We therefore suggest that a 5.7–63 $\mathrm{t\,day^{-1}}$ CO_2 output range may be characteristic of many of the ~ 500 volcanoes active in the Holocene, this in spite the majority lack obvious surface manifestations of degassing. Assuming a representative CO_2 output of $10\,\mathrm{t\,day^{-1}}$ for such 500 Holocene volcanoes, we show that the global population of CO_2 emissions may approach a simple power-law distribution.

Author contribution. M. P. carried out the field campaigns in the study areas and drafted the manuscript. A. A. allowed the work realization and actively contributed to drafting the manuscript. G. G. participated and provided technical support during field campaigns. F. G. provided important suggestions during data processing. V. F. provided technical assistance during the field work. B. B. and E. I. participated and provided technical support during field campaigns in Iceland. All authors have read and approved the final manuscript.

Acknowledgements. The research leading to these results has received funding from the European Research Council under the European Union's Seventh Framework Programme (FP7/2007/2013)/ERC grant agreement n1305377, and from the FP7 grant "Futurevolc". The authors would like to acknowledge technical assistance from Boreal Laser Inc., in particular

Michael Sosef. We also acknowledge IMO (Icelandic Meteorological Office) staff, in particular Melissa Pfeffer and Richard Yeo for support during field work. Nicolas Cristou is thanked for technical assistance during field campaign at Santorini Island. Dario Gharehbaghian, student at University of Bologna, and Lorenza Li Vigni, student at University of Palermo, are acknowledged for their support during field work at Vulcano Island.

References

Aiuppa, A., Federico, C., Giudice, G., and Gurrieri, S.: Chemical mapping of a fumarolic field: La Fossa Crater, Vulcano Island (Aeolian Islands, Italy), Geophys. Res. Lett., 32, L13309, doi:10.1029/2005GL023207, 2005.

Aiuppa, A., Federico, C., Giudice, G., Gurrieri, S., and Valenza, M.: Hydrothermal buffering of the SO_2/H_2S ratio in volcanic gases: evidence from La Fossa Crater fumarolic field, Vulcano Island, Geophys. Res. Lett., 33, L21315, doi:10.1029/2006GL027730, 2006.

Aiuppa, A., Moretti, R., Federico, C., Giudice, G., Gurrieri, S., Liuzzo, M., Papale, P., Shinohara, H., and Valenza, M.: Forecasting Etna eruptions by real-time observation of volcanic gas composition, Geology, 35, 1115–1118, doi:10.1130/G24149A.1, 2007.

Aiuppa, A., Bertagnini, A., Métrich, N., Moretti, R., Di Muro, A., Liuzzo, M., and Tamburello, G.: A model of degassing for Stromboli volcano, Earth Planet. Sc. Lett., 295, 195–204, 2010.

Aiuppa, A., Tamburello, G., Di Napoli, R., Cardellini, C., Chiodini, G., Giudice, G., Grassa, F., and Pedone, M.: First observations of the fumarolic gas output from a restless caldera: implications for the current period of unrest (2005–2013) at Campi Flegrei, Geochem. Geophy. Geosy., 14, 1525–2027, doi:10.1002/ggge.20261, 2013.

Aiuppa, A., Robidoux, P., Tamburello, G., Conde, V., Galle, B., Avard, G., Bagnato, E., De Moor, M., Martinez, M., and Munoz, A.: The Costa Rica–Nicaragua volcanic segment: along-arc variations in volcanic gas chemistry and an improved CO_2 budget, EPSL, submitted, 2014.

Allard, P., Burton, M., and Muré, F.: Spectroscopic evidence for lava fountain driven by previously accumulated magmatic gas, Nature, 433, 407–410, 2005.

Allard, P., Aiuppa, A., Beauducel, F., Calabrese, S., Di Napoli, R., Gaudin, D., Crispi, O., Parello, F., Hammouya, G., and Tamburello, G.: Steam and gas emission rate from La Soufriere volcano, Guadeloupe (Lesser Antilles): implications for the magmatic supply during degassing unrest, Chem. Geol., in press, 2014.

Badalamenti, B., Chiodini, G., Cioni, R., Favara, R., Francofonte, S., Gurrieri, S., Hauser, S., Inguaggiato, S., Italiano, F., Magro, G., Nuccio, P. M., Parello, F., Pennisi, M., Romeo, L., Sortino, F., Valenza, M., and Vurro, F.: Special field workshop at Vulcano (Aeolian Islands) during summer 1998: geochemical result, Acta Vulcanol., 1, 223–227, 1991.
Brantley, S. L. and Koepenick, K. W.: Measured carbon dioxide emissions from Oldoinyo Lengai and shewed distribution of passive volcanic fluxes, Geology, 23, 933–936, 1995.
Brusca, L., Inguaggiato, S., Longo, M., Madonia, P., and Maugeri, R.: The 2002–2003 eruption of Stromboli (Italy): evaluation of the volcano activity by means of continuous monitoring of soil temperature, CO_2 flux, and meteorological parameters, Geochem. Geophy. Geosy., 5, Q12001, doi:10.1029/2004GC000732, 2004.
Burton, M. R., Mader, H. M., and Polacci, M.: The role of gas percolation in quiescent degassing of persistently active basaltic volcanoes, Earth Planet. Sc. Lett., 264, 46–60, 2007.
Burton, M. R., Sawyer, G. M., and Granieri, D.: Deep carbon emissions from volcanoes, Rev. Mineral. Geochem., 75, 323–354, 2013.
Capasso, G., Favara, R., and Inguaggiato, S.: Chemical features and isotopic composition of gaseous manifestations on Vulcano Island (Aeolian Islands, Italy): an interpretative model of fluid circulation, Geochim. Cosmochim. Ac., 61, 3425–3440, 1997.
Capasso, G., Favara, R., Francofonte, S., and Inguaggiato, S.: Chemical and isotopic variations in fumarolic discharge and thermal waters at Vulcano Island (Aeolian Islands, Italy) during 1996: evidence of resumed volcanic activity, J. Volcanol. Geoth. Res., 88, 167–175, 1999.
Carapezza, M. L., Inguaggiato, S., Brusca, L., and Longo, M.: Geochemical precursors of the activity of an open-conduit volcano: the Stromboli 2002–2003 eruptive events, Geophys. Res. Lett., 31, L07620, doi:10.1029/2004GL019614, 2004.
Cardellini, C., Chiodini, G., and Frondini, F.: Application of stochastic simulation to CO_2 flux from soil: mapping and quantification of gas release, J. Geophys. Res., 108, 2425, doi:10.1029/2002JB002165, 2003.
Chiodini, G., Cioni, R., Marini, L., and Panichi, C.: Origin of the fumarolic fluids of Vulcano Island, Italy and implications for volcanic sorveillance, B. Volcanol., 57, 99–110, 1995.
Chiodini, G., Frondini, F., and Raco, B.: Diffuse emission of CO_2 from the Fossa crater, Vulcano Island (Italy), B. Volcanol., 58, 41–50, 1996.
Chiodini, G., Cioni, R., Guidi, M., Raco, B., and Marini, L.: Soil CO_2 flux measurements in volcanic and geothermal areas, Appl. Geochem., 13, 543–552, 1998.

Chiodini, G., Todesco, M., Caliro, S., Del Gaudio, C., Macedonio, G., and Russo, M.: Magma degassing as a trigger of bradyseismic events; the case of Phlegrean Fields (Italy), Geophys. Res. Lett., 30, 8, 1434, doi:10.1029/2002GL01679, 2003.
Chiodini, G., Granieri, D., Avino, R., Caliro, S., Costa, A., and Werner, C.: Carbon dioxide diffuse degassing and estimation of heat release from volcanic and hydrothermal systems, J. Geophys. Res., 110, B08204, doi:10.1029/2004JB003542, 2005.
Chiodini, G., Caliro, S., De Martino, P., Avino, R., and Ghepardi, F.: Early signals of new volcanic unrest at Campi Flegrei caldera? Insights from geochemical data and physical simulations, Geology, 40, 943–946, 2012.
Conde, V., Robidoux, P., Avard, G., et al.: Measurements of SO_2 and CO_2 by combining DOAS, Multi-GAS and FTIR: study cases from Turrialba and Telica volcanoes, Int. J. Earth Sci., in press, doi:10.1007/s00531-014-1040-7, 2014.
De Natale, P., Gianfrani, L., De Natale, G., and Cioni, R.: Gas concentration measurements with DFB lasers to monitor volcanic activity, SPIE Proc. Ser., Applications of Photonic Technology-3, 3491, 783–787, 1998.
Dominey-Howes, D. and Minos-Minopoulos, D.: Perceptions of hazard and risk on Santorini, J. Volcanol. Geoth. Res., 137, 285–310, 2004.
Druitt, T. H., Edwards, L., Mellors, R. M., Pyle, D. M., Sparks, R. S. J., Lanphere, M., Davies, M., and Barreiro, B.: Santorini Volcano, Memoirs, Geological Society, London, 19, 1999.
Favara, R., Giammanco, S., Inguaggiato, S., and Pecoraino, G.: Preliminary estimate of CO_2 output from Pantelleria Island volcano (Sicily, Italy): evidence of active mantle degassing, Appl. Geochem., 16, 883–894, 2001.
Fytikas, M., Kolios, N., and Vougioukalakis, G. E.: Post-Minoan volcanic activity on the Santorini volcano. Volcanic hazard and risk. Forecasting possibilities, in: Thera and the Aegean World III Vol. 2, edited by: Hardy, D. A., Keller, J., Galanopoulos, V. P., Flemming, N. C., and Druitt, T. H., The Thera Foundation, London, 183–198, 1990.
Gianfrani, L., Gagliardi, G., Pesce, G., and Sasso, A.: High sensitivity detection of NO_2 by using a 740 nm semiconductor diode laser, Appl. Phys., B64, 487–491, 1997a.
Gianfrani, L., Gabrysch, M., Corsi, C., and De Natale, P.: Detection of H_2O and CO_2 with distributed feedback diode lasers: measurement of broadening coefficients and assessment of the accuracy levels for volcanic monitoring, Appl. Optics, 36, 9481–9486, 1997b.
Gianfrani, L., De Natale, P., and De Natale, G.: Remote sensing of volcanic gases with a DFB-laser-based fiber spectrometer, Appl. Phys. B-Rapid Common, 70, 467–470, 2000.

Giggenbach, W. F.: Chemical composition of volcanic gases in monitoring and mitigation of volcanic hazards, in: Monitoring and mitigation of volcano hazards, edited by: Scarpa, R. and Tilling, R. I., Springer, Berlin, 221–256, 1996.
Hernández, P. A., Notsu, K., Salazar, J. M., Mori, T., Natale, G., Okada, H., Virgili, G., Shimoike, Y., Sato, M., and Pèrez, N. M.: Carbon dioxide degassing by advective flow from Usu volcano, Japan, Science, 292, 83–86, 2001.
Hilton, D. R., Fisher, T. P., and Marty, B.: Noble gases and volatile recycling at subduction zones, Rev. Mineral. Geochem., 47, 319–370, 2002.
Höskuldsson, Á., Óskarsson, N., Pedersen, R., Grönvold, K., Vogfjörð, K., and Ólafsdóttir, R.: The millennium eruption of Hekla in February 2000, B. Volcanol., 70, 169–182, doi:10.1007/s00445-007-0128-3, 2007.
Ilyinskaya, E., Aiuppa, A., Bergsson, B., Di Napoli, R., Fridriksson, T., Oladottir, A. A., Oskarsson, F., Grassa, F., Pfeffer, M., Lechner, K., Yeo, R., and Giudice, G.: Degassing regime of Hekla volcano 2012–2013, Geochim. Cosmochim. Ac., accepted, 2014.
Inguaggiato, S., Martin-Del Pozzo, A. L., Aguayo, A., Capasso, G., and Favara, R.: Isotopic, chemical and dissolved gas constraints on spring water from Popocatépetl (Mexico): evidence of gas-water interaction magmatic component and shallow fluids, J. Volcanol. Geoth. Res., 141, 91–108, 2005.
Inguaggiato, S., Vita, F., Rouwet, D., Bobrowski, N., Morici, S., and Sollami, A.: Geochemical evidence of the renewal of volcanic activity inferred from CO_2 soil and SO_2 plume fluxes: the 2007 Stomboli eruption (Italy), B. Volcanol., 73, 443–456, 2011.
Inguaggiato, S., Mazot, A., Diliberto, I. S., Inguaggiato, C., Madonia, P., Rouwet, D., and Vita, F.: Total CO_2 output from Vulcano island (Aeolian Islands, Italy), Geochem. Geophy. Geosy., 13, Q02012, doi:10.1029/2011GC003920, 2012.
Isaaks, E. H. and Srivastava, R. M.: An Introduction to Applied Geostatistics, Oxford University Press, New York, 561 pp., 1989.
ISMOSAV: Website of the Institute for the Study and Monitoring of the Santorini Volcano, available at: http://ismosav.santorini.net/, 2009.
Larsen, G., Dugmore, A. J., and Newton, A. J.: Geochemistry of historical-age silicic tephras in Iceland, Holocene, 9, 463–471, 1999.
Markússon, S. H. and Stefánsson, A.: Geothermal surface alteration of basalts, Krýsuvík Iceland – alteration mineralogy, water chemistry and the effects of acid supply on the alteration process, J. Volcanol. Geoth. Res., 206, 46–59, 2011.

Marret, R. and Almendinger, R. W.: Estimates of strain due to brittle faulting: sampling of fault populations, J. Struct. Geol., 13, 735–738, 1991.
Mazot, A., Rouwet, D., Taran, Y., Inguaggiato, S., and Varley, N.: CO_2 and He degassing at El Chichón volcano (Chiapas, Mexico): gas flux, origin, and relationship with local and regional tectonics, B. Volcanol., 73, 423–441, doi:10.1007/s00445-010-0443-y, 2011.
McGonigle, A. J. S., Aiuppa, A., Giudice, G., Tamburello, G., Hodson, A. J., and Gurrieri, S.: Unmanned aerial vehicle measurements of volcanic carbon dioxide fluxes, Geophys. Res. Lett., 35, L06303, doi:10.1029/2007GL032508, 2008.
Mori, T., Shinohara, H., Kazahaya, K., Hirabayashi, J., Matsushima, T., Mori, T., Ohwada, M., Odai, M., Iino, H., and Miyashita, M.: Time-averaged SO_2 fluxes of subduction-zone volcanoes: example of a 32-year exhaustive survey for Japanese volcanoes, J. Geophys. Res., 118, 8662–8674, 2013.
Newman, A. V., Stiros, S., Feng, L., Psimoulis, P., Moschas, F., Saltogianni, V., Jiang, Y., Papazachos, C., Panagiotopoulos, D., Karagianni, E., and Vamvakaris, D.: Recent geodetic unrest at Santorini Caldera, Greece, Geophys. Res. Lett., 39, L06309, doi:10.1029/2012GL051286, 2012.
Oppenheimer, C., Lomakina, A., Kyle, P. R., Kingsbury, N. G., and Boichu, M.: Pulsatory magma supply to a phonolite lava lake, Earth Planet. Sc. Lett., 284, 392–398, 2009.
Oppenheimer, C., Moretti, R., Kyle, P. R., Eschenbacher, A., Lowenstern, J. B., Hervig, R. L., and Dunber, N. W.: Mantle to surface degassing of alkalic magmas at Erebus volcano, Antarctica, Earth Planet. Sc. Lett., 306, 261–271, 2011.
Paonita, A., Favara, R., Nuccio, P. M., and Sortino, F.: Genesis of fumarolic emissions as inferred by isotope mass balances: CO_2 and water at Vulcano Island, Italy, Geochim. Cosmochim. Ac., 66, 759–772, 2002.
Paonita, A., Federico, C., Bonfanti, P., Capasso, G., Inguaggiato, S., Italiano, F., Madonia, P., Pecoraino, G., and Sortino, F.: The episodic and abrupt geochemical changes at La Fossa fumaroles (Vulcano Island, Italy) and related constraints on the dynamics, structure, and compositions of the magmatic system, Geochim. Cosmochim. Ac., 120, 158–178, 2013.
Papazachos, B. C., Dimitriadis, S. T., Panagiotopoulos, D. G., Papazachos, C. B., and Papadimitriou, E. E.: Deep structure and active tectonics of the southern Aegean volcanic arc, Dev. Volcano., 7, 47–64, 2005.
Parks, M. M., Biggs, J., England, P., Mather, T. A., Nomikou, P., Palamartchouk, K., Papanikolaou, X., Paradissis, D., Parsons, B., Pyle, D. M., Raptakis, C., and Zacharis, V.: Evolution of

Santorini volcano dominated by episodic and rapid fluxes of melt from depth, Nat. Geosci., 5, 749–754, 2012.
Parks, M. M., Caliro, S., Chiodini, G., Pyle, D. M., Mather, T. A., Berlo, K., Edmonds, M., Biggs, J., Nomikou, P., and Raptakis, C.: Distinguishing contributions to diffuse CO_2 emissions in volcanic areas from magmatic degassing and thermal decarbonation using soil gas ^{222}Rn–$\delta^{13}C$ systematics: application to Santorini volcano, Greece, Earth Planet. Sc. Lett., 377–378, 180–190, 2013.
Pecoraino, G., Brusca, L., D'Alessandro, W., Giammanco, S., Inguaggiato, S., and Longo, M.: Total CO_2 output from Ischia Island volcano (Italy), Geochem. J., 39, 451–458, doi:10.2343/geochemj.39.451, 2005.
Pedone, M., Aiuppa, A., Giudice, G., Grassa, F., Cardellini, C., Chiodini, G., and Valenza, M.: Volcanic CO_2 flux measurement at Campi Flegrei by Tunable Diode Laser Absorption Spectroscopy, B. Volcanol., 76, 812, doi:10.1007/s00445-014-0812-z, 2014.
Richter, D., Erdelyi, M., Curl, R. F., Tittel, F. K., Oppenheimer, C., Duffell, H. J., and Burton, M.: Field measurements of volcanic gases using tunable diode laser based mid-infrared and Fourier transform infrared spectrometers, Opt. Laser. Eng., 37, 171–186, 2002.
Shinohara, H.: Volatile flux from subduction zone volcanoes: insights from a detailed evaluation of the fluxes from volcanoes in Japan, J. Volcanol. Geoth. Res., 268, 46–63, 2013.
Siebert, L. and Simkin, T.: Volcanoes of the World: an Illustrated Catalog of Holocene Volcanoes and their Eruptions, Smithsonian Institution Digital Information Series GVP-3, available at: http://www.volcano.si.edu/world, 2002.
Sigmarsson, O., Condomines, M., and Fourcade, S.: A detailde Th, Sr and O isotope study of Hekla: differentiation processes in an Icelandic volcano, Contrib. Mineral. Petr., 112, 20–34, 1992.
Smithsonian Institution: available at: http://www.volcano.si.edu/data_criteria.cfm, 2013.
Tamburello, G., Kantzas, E. P., McGonigle, A. J. S., Aiuppa, A., and Giudice, G.: UV camera measurements of fumarole field degassing (La Fossa crater, Vulcano Island), J. Volcanol. Geoth. Res., 199, 47–52, 2011.
Tamburello, G., Hansteen, T. H., Bredemeyer, S., Aiuppa, A., and Giudice, G.: Gas fluxes and compositions of two active volcanoes in northern Chile: Lascar and Lastarria, American Geophysical Union Fall Meeting 2013, abstract #V31B-2703, 2013.
Tassi, F., Vaselli, O., Papazachos, C., Giannini, L., Chiodini, G., Vougioukalakis, G. E., Karagianni, E., Vamvakaris, D., and Panagiotopoulos, D.: Geochemical and isotopic changes

in the fumarolic and submerged gas discharge during the 2011–2012 unrest at Santorini caldera (Greece), B. Volcanol., 75, 711, doi:10.1007/s00445-013-0711-8, 2013.
Thorarinsson, S.: The eruption of Hekla 1947–48, Soc. Sci. Isl., 1–183, 1967.
Thordarson, T. and Larsen, G.: Volcanism in Iceland in historical time: volcano types, eruption styles and eruptive history, The eruption of Hekla 1947-1948, I. The eruptions of Hekla in historical times, A tephrochronological study. Visindafelag Islendinga, Reykjavik, J. Geodyn., 43, 118–152, 2007.
Trottier, S., Gunter, W. D., Kadatz, B., Olson, M., and Perkins, E. H.: Atmospheric monitoring for the Pembina Cardium CO_2 Monitoring Project using open path laser technology, Science Direct Energy Procedia, 1, 2307–2314, doi:10.1016/j.egypro.2009.01.300, 2009.
Tsapanos, T. M., Galanopoulos, D., and Burton, P. W.: Seismicity in the Hellenic Volcanic Arc: relation between seismic parameters and the geophysical fields in the region, Geophys. J. Int., 117, 677–694, 1994.
Tulip, J.: Gas Detector, United States Patent, 5,637,872 250/338.5, 1997.
Turcotte, D. L.: Fractals and Chaos in Geology and Geophysics, Cambridge University Press, 52–64, 1992.
Vougioukalakis, G. E., Mitropoulos, D., Perissoratis, C., Andrinopoulos, A., and Fytikas, M.: The submarine volcanic centre of Coloumbo, Santorini, Greece, Bull. Soc. Geol. Greece XXX, 3, 351–360, 1994.
Werner, C. and Cardellini, C.: Comparison of carbon dioxide emissions with fluid upflow, chemistry, and geologic structures at the Rotorua geothermal system, New Zealand, Geothermics, 35, 221–238, doi:10.1016/j.geothermics.2006.02.2006, 2006.

Table 1. CO_2 fluxes (in t day^{-1}) and standard deviation (1 σ) calculated in this study. The plume transport vertical speed (in m s^{-1}) is also given for each site.

Volcano	Date	Gas speed (m s^{-1}) ($\pm 1\,\sigma$)	CO_2 Flux (t d^{-1}) ($\pm 1\,\sigma$)
Nea Kameni	9 Apr 2013	1.20 ± 0.4	63 ± 22
Hekla	2 Jul 2013	1.00 ± 0.5	15 ± 7
Krýsuvík	5 Jul 2013	1.17 ± 0.18	5.7 ± 0.9
Vulcano	11 Mar 2014	1.00 ± 0.20	524 ± 108

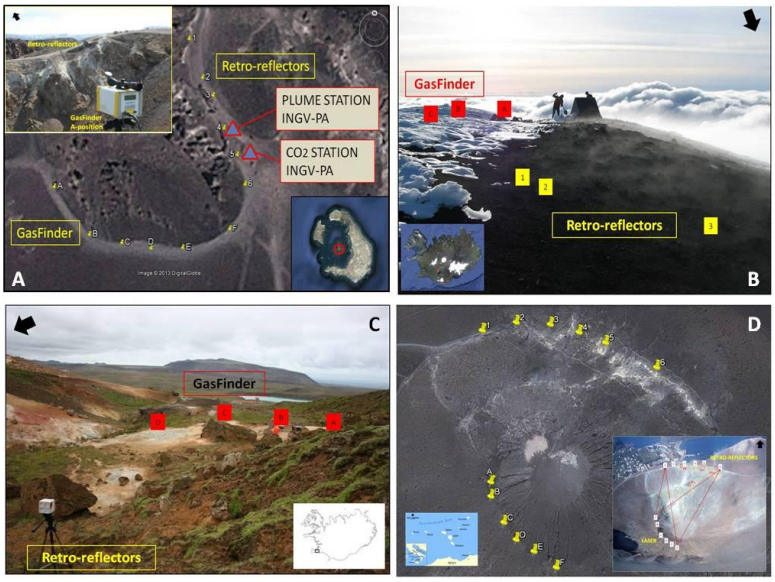

Figure 1. The study areas. **(A)** Nea Kameni summit crater (Greece) **(B)** Hekla summit (Iceland) **(C)** Krýsuvík hydrothermal field **(D)** "La Fossa" crater (Vulcano Island). In each picture, the positions of GasFinder and retro-reflectors are shown with letters and numbers, respectively.

Discussion Paper | Discussion Paper | Discussion Paper | Discussion Paper |

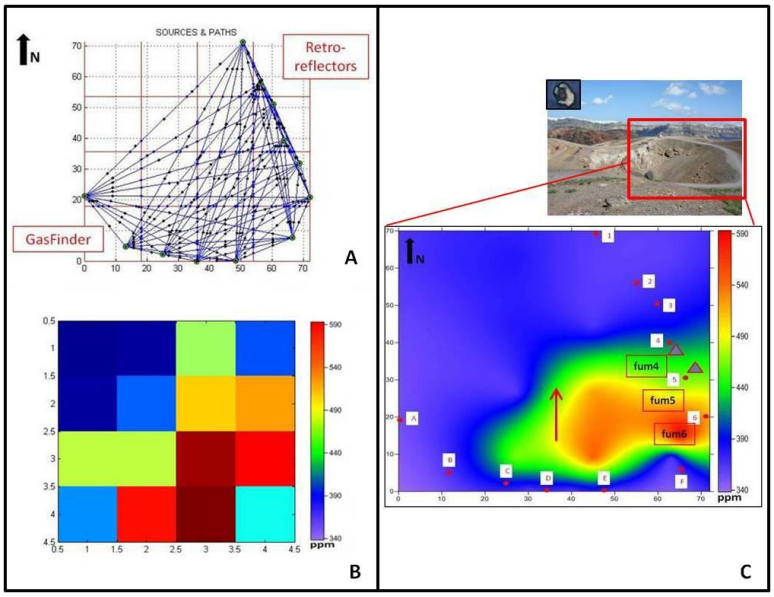

Figure 2. Output of the tomographic algorithm. Example for the Nea Kameni campaign, 9 April 2013. **(A)** Geometric reconstruction of the field experimental set-up and **(B)** tomographic matrix. The script uses a data inversion procedure to assign an averaged CO_2 mixing ratio (in ppm) to each cell of the matrix. **(C)** CO_2 mixing ratios (ppm) contour map. GasFinder and retro-reflectors positions are shown with letters and numbers respectively. "Fum4", "Fum5" and "Fum6": positions of main degassing vents; blue triangles: permanent INGV-PA stations; red arrow: principal direction of plume dispersal. See text.

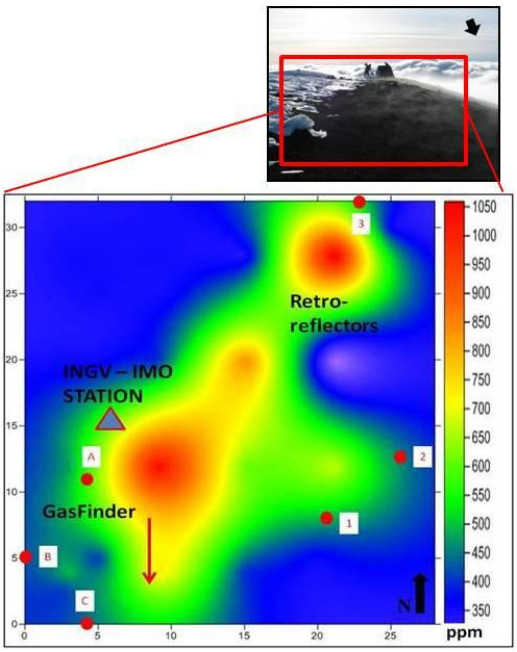

Figure 3. Contour map of CO_2 mixing ratios (ppm), Hekla campaign of 2 July 2013. GasFinder and retro-reflectors positions are shown with letters and numbers respectively. Blue triangle: INGV-PA/IMO station; red arrow: principal direction of plume dispersal.

Discussion Paper | Discussion Paper | Discussion Paper | Discussion Paper |

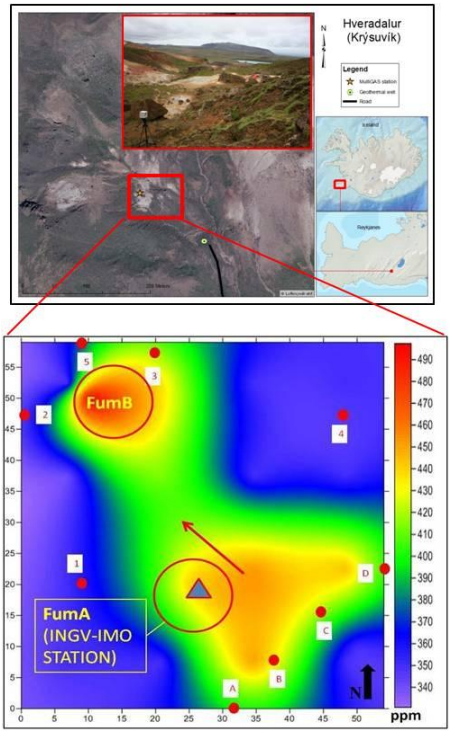

Figure 4. CO_2 Contour map of CO_2 mixing ratios (ppm), Krýsuvík campaign of 5 July 2013. GasFinder and retro-reflectors positions are shown with letters and numbers respectively. "FumA" and "FumB": positions of main degassing vents; blue triangle: INGV-PA/IMO station; red arrow: principal direction of plume dispersal.

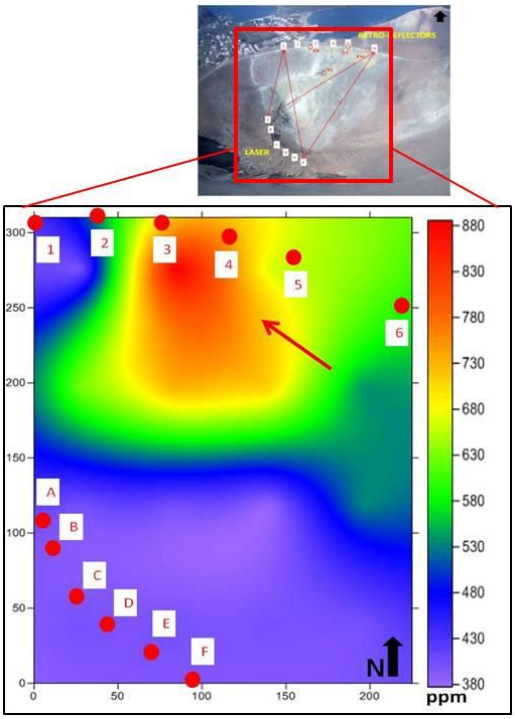

Figure 5. Contour map of CO_2 mixing ratios (ppm), "La Fossa" campaign, Vulcano Island, 11 March 2014. GasFinder and retro-reflectors positions are shown with letters and numbers respectively. Red arrow: principal direction of plume dispersal.

Discussion Paper | Discussion Paper | Discussion Paper | Discussion Paper |

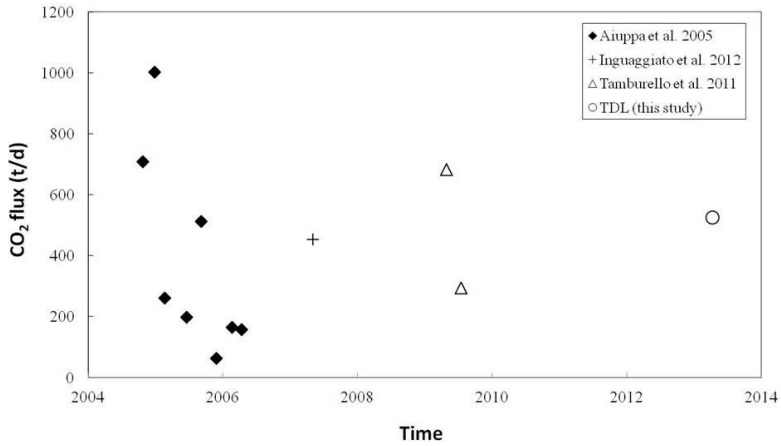

Figure 6. Time-series of CO_2 flux values (tons/day) for "La Fossa crater" (Vulcano Island). Previous works: Aiuppa et al. (2005, 2006), Tamburello et al. (2011) and Inguaggiato et al. (2012). The flux value of $524 \pm 108\,t\,d^{-1}$, obtained in this study, is also shown.

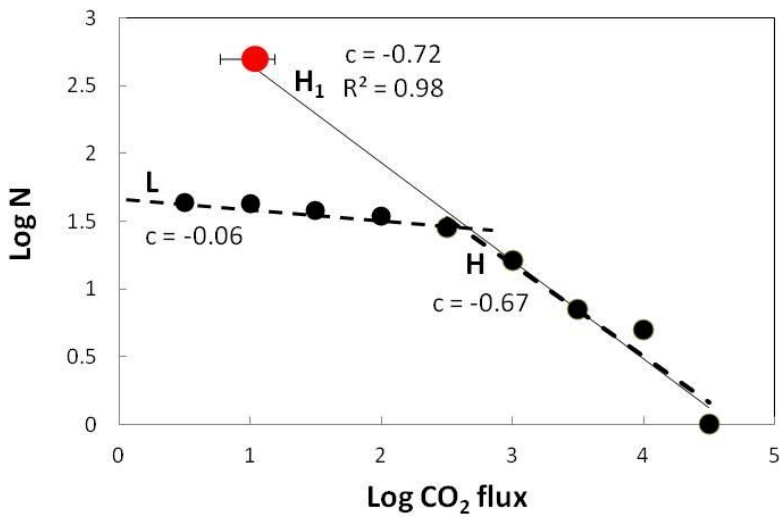

Figure 7. Cumulative frequency of the number of volcanoes (N) emitting CO_2 flux $\geq f$ (in logarithmic scale). The diagram is based upon the dataset of Burton et al. (2013), implemented with new results from this study and additional data (see text). Red point, with coordinates $\log f = 1$ (CO_2 flux $= 10\,t\,day^{-1}$) and $\log N = 2.69$ (500 volcanoes), lies right above the linear regression line of the high CO_2 flux ($\log f > 2.5$) population (dashed line H). The regression line (line H_1; $R^2 = 0.98$) is obtained considering the high CO_2 flux volcanoes ($\log f \geq 2.5$) plus this new $\log f = 1$ point.

Discussion Paper | Discussion Paper | Discussion Paper | Discussion Paper |